

## Role of the Mitochondrial Signaling Pathway in Murine Coronavirus-Induced Oligodendrocyte Apoptosis

Yin Liu, Yinghui Pu, and Xuming Zhang\*

*Department of Microbiology and Immunology, University of Arkansas for Medical Sciences, Little Rock, Arkansas 72205-7199*

Received 26 May 2005/Accepted 13 October 2005

**A previous study demonstrated that infection of rat oligodendrocytes by mouse hepatitis virus (MHV) resulted in apoptosis, which is caspase dependent (Y. Liu, Y. Cai, and X. Zhang, *J. Virol.* 77:11952–11963, 2003). Here we determined the involvement of the mitochondrial pathway in MHV-induced oligodendrocyte apoptosis. We found that caspase-9 activity was 12-fold higher in virus-infected cells than in mock-infected cells at 24 h postinfection (p.i.). Pretreatment of cells with a caspase-9 inhibitor completely blocked caspase-9 activation and partially inhibited the apoptosis mediated by MHV infection. Analyses of cytochrome *c* release further revealed an activation of the mitochondrial apoptotic pathway. Stable overexpression of the two antiapoptotic proteins Bcl-2 and Bcl-xL significantly, though only partially, blocked apoptosis, suggesting that activation of the mitochondrial pathway is partially responsible for the apoptosis. To identify upstream signals, we determined caspase-8 activity, cleavage of Bid, and expression of Bax and Bad by Western blotting. We found a drastic increase in caspase-8 activity and cleavage of Bid at 24 h p.i. in virus-infected cells, suggesting that Bid may serve as a messenger to relay the signals from caspase-8 to mitochondria. However, treatment with a caspase-8 inhibitor only slightly blocked cytochrome *c* release from the mitochondria. Furthermore, we found that Bax but not Bad was significantly increased at 12 h p.i. in cells infected with both live and UV-inactivated viruses and that Bax activation was partially blocked by treatment with the caspase-8 inhibitor. These results thus establish the involvement of the mitochondrial pathway in MHV-induced oligodendrocyte apoptosis.**

Apoptosis or programmed cell death is an important biologic process that regulates homeostasis, tissue development, and the immune system. Cell death by apoptosis is characterized by chromatin condensation, cell shrinkage, membrane blebbing, and DNA fragmentation (19, 20, 32). Apoptosis can be triggered by diverse intrinsic and extrinsic signals, including virus infection. Initiation of apoptosis usually follows cascades of signaling events or apoptotic pathways upon receipt of a variety of apoptotic signals. The most common apoptotic pathway is the “death” receptor-mediated signaling pathway, which involves interactions of apoptotic factors with either cell surface molecules such as Fas (CD95) or Fas ligand and tumor necrosis factor receptor (TNFR) or TNF or adaptor proteins such as Fas-associated death domain (FADD) or TNFR-associated death domain (TRADD), as well as activation of initiator caspases such as caspase-8 and -10 and of effector caspases such as caspase-3, -6, and -7, ultimately leading to apoptosis (4, 11, 19, 24, 34). Another well-characterized apoptotic pathway is the mitochondrion-mediated pathway, which can be activated by either extracellular or intracellular death signals and which can be largely controlled by the two master antiapoptotic proteins of the mitochondria, Bcl-2 and Bcl-xL (24, 27). Activation of initiator caspase-8 and -10 can also activate the mitochondrial apoptotic pathway via cleavage of Bid (a member of the proapoptotic Bcl-2 family) and translocation of the trun-

cated Bid to mitochondria (29). Many proapoptotic members of the Bcl-2 family such as Bax and Bad can relay upstream apoptotic signals to the mitochondria (12, 22, 33). Activation of the mitochondrial pathway triggers cytochrome *c* release, which then interacts with Apaf-1. The cytochrome *c*/Apaf-1 complex in turn activates the initiator caspase-9 and subsequently the effector caspase-3, leading to apoptosis (4).

Mouse hepatitis virus (MHV) is a prototype of murine coronavirus. It is an enveloped RNA virus that can infect rodents and cause enteritis, hepatitis, and central nervous system (CNS) diseases. Depending on the genetic background of the virus strains and the host, the CNS diseases caused by MHV infection can vary significantly, ranging from acute fatal encephalitis to persistent infections with or without chronic demyelination (23). In the CNS of susceptible mice, acute demyelination can be seen as early as 7 days postinfection (p.i.). If the mice survive the acute phase, demyelination can peak by 4 to 6 weeks p.i. and continues to be detectable after 1 year, although infectious virus is not detectable after about 4 weeks (6, 13, 14).

The precise mechanism of CNS demyelination caused by MHV infection is not known. Experimental evidence strongly suggests that the immune components play an important role in initiation and progression of a robust CNS demyelination disease following MHV infection (5, 7, 10, 28, 30, 31). In addition, apoptotic oligodendrocytes have been detected in the vicinity of demyelinating lesions of MHV-infected mice and rats (1, 21, 31). However, until recently the question as to whether the observed oligodendrocyte apoptosis results directly from virus infection in oligodendrocytes or indirectly

\* Corresponding author. Mailing address: Department of Microbiology and Immunology, University of Arkansas for Medical Sciences, 4301 W. Markham St., Slot 511, Little Rock, AR 72205-7199. Phone: (501) 686-7415. Fax: (501) 686-5359. E-mail: zhangxuming@uams.edu.

from the attack by molecules secreted from other CNS resident or infiltrated cells during virus infection has not been addressed. In a previous study, we demonstrated for the first time that infection of cultured rat oligodendrocytes by MHV resulted in apoptotic cell death and that MHV-induced oligodendrocyte apoptosis was caspase dependent (16).

In the present study, we determined the involvement of the mitochondrion-mediated apoptotic pathway in MHV-induced oligodendrocyte apoptosis. We found a significant activation of caspase-9 activity and an increased amount of cytochrome *c* released from mitochondria of MHV-infected cells. Furthermore, overexpression of Bcl-2 and Bcl-xL significantly inhibited MHV-induced apoptosis. Although caspase-8 activation and cleavage of Bid occurred in MHV-infected cells, experiments with caspase-8 inhibitor and detection of proapoptotic proteins suggest that Bax activation likely plays an important role in activation of the MHV-induced mitochondrial apoptotic pathway. Our results thus establish that the mitochondrial apoptotic pathway is involved in the regulation of MHV-induced oligodendrocyte apoptosis.

#### MATERIALS AND METHODS

**Cells, virus, and reagents.** The CG-4 cell is a permanent, undifferentiated type 2 oligodendrocyte or astrocyte progenitor cell that was originally established during a primary neural cell culture derived from the brains of newborn Sprague-Dawley rat pups (1 to 3 days postnatal) (18). It was kindly provided by Paul Drew (University of Arkansas for Medical Sciences). On a conditional culture medium, the CG-4 cell maintains its undifferentiated progenitor phenotype indefinitely (16). Under a defined culture condition, CG-4 cells differentiated into mature oligodendrocytes, as evidenced by the appearance of myelin basic protein (16). Mature oligodendrocytes were used for virus infection throughout this study. Mouse astrocytoma DBT cells (9) were cultured in Eagle's minimum essential medium and used for virus propagation and virus plaque assay (16). Mouse hepatitis virus strain JHM was obtained from Michael Lai's laboratory. It was derived from JHM (3) after 15 passages of undiluted virus propagations in cell culture. This culture-adapted virus has been continuously passaged over the years. It has a severe cytopathic effect in DBT cells. It induced apoptosis in CG-4 differentiated oligodendrocytes in a previous study (16). The virus preparation was purified through a sucrose cushion, and virus titer was determined by plaque assay as described previously (16). Caspase-8 inhibitor (2-Ile-Glu-Thr-Asp-CH<sub>2</sub>F) and caspase-9 inhibitor (2-Leu-Glu-His-Asp-CH<sub>2</sub>F) were purchased from CalBiochem and dissolved in dimethyl sulfoxide (DMSO). Their cytotoxicity was determined in oligodendrocytes, and a noncytotoxic concentration was used for all subsequent experiments.

**Plasmid construction, DNA transfection, and selection of stable transfectants.** The plasmid containing Bcl-2 open reading frame (ORF) was kindly provided by Marie Hardwick (The Johns Hopkins University), and the Bcl-2 ORF was subcloned into the eukaryotic expression vector pcDNA3 (Clontech Laboratories, Inc.), resulting in pcDNA3/Bcl-2. The construction of an expression vector containing the Bcl-xL ORF (pcDNA3/Bcl-xL) was described previously (15). CG-4 cells were grown in 60-mm culture plates (Sarsted) to ~60% confluence and were transfected with plasmid DNA pcDNA3/Bcl-xL, pcDNA3/Bcl-2, or pcDNA3 vector using the cationic liposome transfection reagent FuGene-6 according to the manufacturer's instructions (Roche Applied Science). Briefly, 1 µg of each construct was mixed with 6 µl of FuGene-6 in 100 µl of serum-free Dulbecco's modified Eagle's medium. The mixture was then added to CG-4 cells. Following incubation for 24 h, Geneticin (G418) (GIBCO-BRL) was added to the medium at a final concentration of 400 µg/ml, and the cells were grown for 2 to 3 days. Cells that died off during this period were removed, while surviving cells were allowed to grow further in the presence of G418 with replenishment of fresh medium every 3 days. Cells that were resistant to G418 treatment for 4 weeks were screened for expression of Bcl-2 and Bcl-xL by Western blotting using a rabbit antiserum to Bcl-2 peptide (N19:SC-492; 1:1,000 dilution; Santa Cruz Biotechnology, Inc.) and a monoclonal antibody to Bcl-xL (1:1,000 dilution; Cell Signaling), respectively.

**Assay for caspase activity.** Cells were grown in 60-mm dishes and either mock infected with Eagle's minimum essential medium or infected with MHV at a multiplicity of infection (MOI) of 5. Cells were collected at various time points

p.i. by scraping, split into a 96-well plate, and spun down at 500 × *g* for 5 min. Following removal of supernatant, lysis of cells and determination of caspase activities were carried out with a fluorometric caspase assay kit (caspase-9 activity assay kit QIA72 and caspase-8 activity assay kit QIA71; Oncogene Research Products) according to the manufacturer's instructions. Briefly, 50 µl of the extraction buffer was added to each well and the plate was incubated at 4°C for 30 min. Fifty microliters of the assay buffer was then added to each well followed by incubation of the plate at 37°C for 30 min. After addition of caspase-8 and -9 fluorescent substrate conjugates (10 µl/well) and incubation at 37°C for 2 h, the plate was read with a fluorescent plate reader (Spectra Max M2; Molecular Device) capable of measuring excitation at ~400 nm and emission at ~505 nm.

**TUNEL.** Terminal deoxynucleotidyl transferase-mediated dUTP-fluorescein nick end labeling (TUNEL) was performed with the fluorescein-FragEL DNA fragmentation detection kit according to the manufacturer's instructions (Oncogene Research Products, Biosciences Inc.). Briefly, cells were fixed with 4% paraformaldehyde at room temperature for 10 min. After being washed with phosphate-buffered saline (PBS), cells were treated with proteinase K (2 mg/ml) at room temperature for 5 min followed by addition of 100 µl 1 × TdT equilibration buffer for 30 min. The cells were then stained with the fluorescein-FragEL-TdT labeling reaction mix (57 µl) and 3 µl TdT enzyme at 37°C for 1 h. Following washing with Tris-buffered saline (TBS), the cells were subjected to flow cytometric analysis. The data were analyzed with the software WinMDI2.8.

**Cytochrome *c* release assay.** The cytochrome *c* release apoptosis assay kit (Calbiochem; catalog no. QIA87) was used for detection of cytochrome *c* according to the manufacturer's instructions. Briefly, cells were collected from culture dishes by scraping and by centrifugation at 600 × *g* for 5 min at 4°C. Cells were resuspended in 1 ml of 1 × cytosol extraction buffer, incubated on ice for 10 min, and homogenized in an ice-cold tissue grinder. Cell homogenate was subjected to low-speed centrifugation (700 × *g*) for 10 min at 4°C. The resultant supernatant was further centrifuged at a higher speed (10,000 × *g*) for 30 min at 4°C. Supernatants from the high-speed centrifugation were used as the cytosolic fraction, while the pellets, which were then resuspended in 100 µl of the mitochondrial extraction buffer, were used as the mitochondrial fraction. Cell number equivalents (10<sup>5</sup> cells) or the same protein concentrations (10 µg) of each cytosolic and mitochondrial fraction were analyzed by Western blotting following separation by sodium dodecyl sulfate-polyacrylamide gel electrophoresis (SDS-PAGE) on a 10% gel.

**Assay for apoptosis with annexin V.** Cells were infected with MHV at an MOI of 10 or mock infected as a control. At 12 h p.i., approximately 1 × 10<sup>5</sup> cells were collected by centrifugation. To determine apoptosis, cells were resuspended in 500 µl of 1 × annexin V binding buffer and incubated with 1 µl of the annexin V-enhanced green fluorescence protein (EGFP) at room temperature for 5 min in the dark using the assay kit according to the manufacturer's instruction (Bio Vision Inc., Mountain View, CA). Cells were then analyzed by flow cytometry using the FL1 channel for detection of annexin V-EGFP.

**Western blot analysis.** For detection of cellular proteins, oligodendrocytes were either infected with MHV or mock infected. At various time points p.i., cells were lysed with radioimmunoprecipitation assay buffer (50 mM Tris-HCl, pH 7.5, 150 mM NaCl, 0.5% sodium deoxycholate, 1% Nonidet P-40) containing protease inhibitor cocktail tablets (Roche, Mannheim, Germany). The cell lysates were passed through a 25-gauge needle several times to shear the DNA and were clarified from cell debris by centrifugation. The protein concentration was measured by using a Bio-Rad protein assay kit (Bio-Rad, Richmond, CA). Cellular proteins with equivalent numbers of cells for each sample were resuspended in 20 µl of Lammeli's electrophoresis sample buffer (10 mM Tris-HCl, pH 6.8, 100 mM dithiothreitol, 2% SDS, 0.1% bromophenol blue, 10% glycerol), boiled for 5 min, and resolved by SDS-PAGE on 12% gel. Proteins were then transferred to nitrocellulose membrane (MSI, Westborough, MA) overnight at 50 V in a transfer buffer (25 mM Tris, 200 mM glycine, 20% methanol, 0.02% SDS). After blocking with 5% skim milk in TBS for 1 h at room temperature, nitrocellulose membrane was washed three times in TBS containing 0.1% Tween 20 and detected with a protein-specific antibody for 2 h at room temperature followed by a secondary goat anti-rabbit immunoglobulin G antibody or anti-mouse immunoglobulin G antibody coupled to horseradish peroxidase (1:2,000 dilution) (Sigma) for 1 h at room temperature. The primary antibodies used in this study include a polyclonal rabbit antibody specific to Bax (Ab-1) (1 µg/ml) (catalog no. PC66; Calbiochem), a polyclonal rabbit antibody specific to Bad (1:1,000 dilution) (catalog no. SC943; Santa Cruz Biotechnology Inc.), a monoclonal antibody specific to cytochrome *c* (1 µg/ml), and a monoclonal antibody specific to β-actin as an internal control (1:2,500) (Sigma). The presence of the specific proteins was visualized with the enhanced chemiluminescence (ECL) system using peracid as a substrate (Amersham Pharmacia

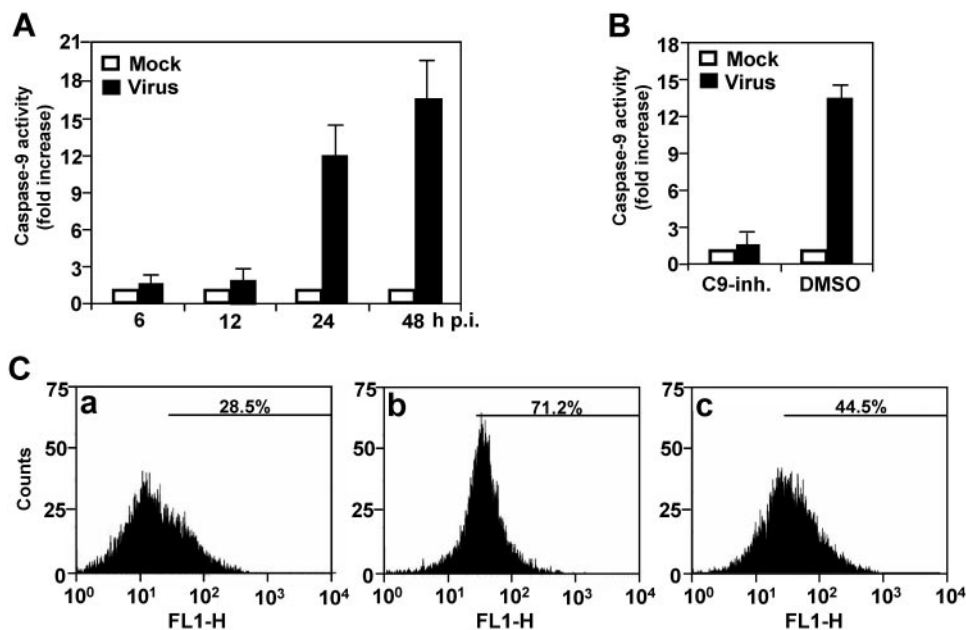


FIG. 1. Activation of caspase-9 in oligodendrocytes by MHV infection. (A) Caspase-9 activity. Cells were infected with MHV at an MOI of 5. At various time points p.i. as indicated, cell extract was prepared and cleavage of pro-caspase-9 and the presence of the active caspase-9 were detected with a caspase colorimetric protease assay kit using specific substrates as described in Materials and Methods. The caspase-9 activity from virus-infected cells was expressed as means  $\pm$  SD from three independent experiments and as fold increase over that from the mock-infected control, which was set as onefold. (B) Effect of caspase-9 inhibitor I (C9-inh.) on caspase-9 activity. Cells were treated with cell-permeable caspase-9 inhibitor I 1 h prior to and during virus infection for 24 h or with DMSO as a negative control. Mock-infected cells were used for normalizing the caspase-9 activity expressed as fold increase as described for panel A. (C) TUNEL with FragEL DNA fragmentation detection kit (Oncogene Research Products) using terminal deoxynucleotidyl transferase (TdT) in (a) mock-infected, (b) MHV-infected, and (c) MHV-infected and caspase-9 inhibitor I-treated cells at 48 h p.i. The fluorescence end labeling was quantified by flow cytometry, and the percentage of the TUNEL-positive signal was indicated in each panel. For statistical analysis, data from three independent experiments were analyzed and compared between each pair. FL1-H, fluorescence intensity; counts, cell counts.

Biotech) followed by autoradiography with exposure times ranging from 30 s to 5 min.

**Statistical analysis.** The results are expressed as the mean  $\pm$  standard deviation (SD), and the mean values were compared by using Student's *t* test. Values of  $P < 0.05$ ,  $P < 0.01$ , and  $P < 0.001$  were considered statistically significant.

## RESULTS

**Activation of caspase-9 in MHV-infected rat oligodendrocytes.** Using a pan-caspase-inhibitor, ZVAD-fmk, we previously showed that MHV-induced apoptosis of oligodendrocytes is caspase dependent (16). To identify the apoptotic signaling pathway, we determined the activity of caspase-9 in MHV-infected oligodendrocytes. The result showed that the caspase-9 activity increased slightly at 6 and 12 h p.i. in MHV-infected cells as compared to that of mock-infected cells, but the increase was statistically insignificant ( $P > 0.5$ ) (Fig. 1A). It increased significantly to approximately 12-fold higher in virus-infected cells than in mock-infected cells at 24 h p.i. ( $P < 0.01$ ), and the difference continued to increase to 16.5-fold at 48 h p.i. (Fig. 1A). This result demonstrates that caspase-9 is activated by MHV infection. To confirm that the determined caspase activity is specific for caspase-9, cells were pretreated with caspase-9 inhibitor (80  $\mu$ M) for 2 h or with DMSO as a negative control. Cells were then infected with MHV or mock infected with PBS. At 24 h p.i., we again determined the caspase activity. We found that the caspase-9 activity was completely inhibited by the caspase-9 inhibitor but not by DMSO

(Fig. 1B), thus establishing the specificity of the caspase-9 activation.

To evaluate the functional relevance of the caspase-9 activation to the observed apoptosis, we performed TUNEL to detect nicked DNAs, a hallmark of apoptosis, in infected oligodendrocytes. As shown in Fig. 1C, 28.5% of the cells exhibited TUNEL fluorescence staining in mock-infected cells, as revealed by flow cytometry, whereas 71.2% of the cells had significant TUNEL staining in virus-infected cells. These data are consistent with our previous results obtained with propidium iodide staining (16). When the cells were treated with the caspase-9 inhibitor, the percentage of TUNEL-positive infected cells decreased to 44.5%. The differences between each group were statistically significant ( $P < 0.01$ ). These results indicate that caspase-9 activation plays a role in MHV-induced oligodendrocyte apoptosis.

**Release of cytochrome *c* from mitochondria of MHV-infected oligodendrocytes.** Since the mitochondrial pathway usually plays a major role in activation of caspase-9 and since the activation of mitochondrial pathway triggers the release of cytochrome *c*, we then determined cytochrome *c* release. Cells were infected with MHV or mock infected with PBS. At various time points postinfection, cells were lysed with a cytosol extraction buffer, and the cytosolic and mitochondrial fractions were separated by differential centrifugation. The proteins were then separated by SDS-PAGE and detected by Western blotting with a cytochrome *c*-specific antibody. As shown in

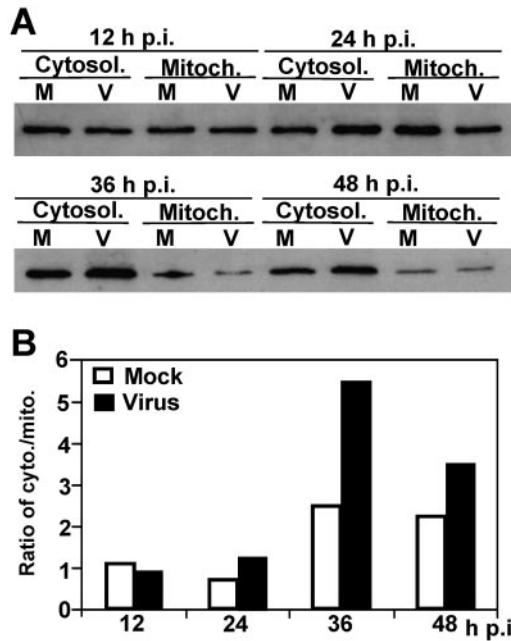


FIG. 2. Release of cytochrome *c* from mitochondria by MHV infection. (A) Cells were infected with MHV (V) or mock infected with PBS (M). At various time points p.i., as indicated at the top of the figure, cells were harvested and the cytosolic (Cytosol.) and mitochondrial (Mitoch.) fractions were separated by differential centrifugation using the cytochrome *c* release assay kit as described in Materials and Methods. Proteins were separated by SDS-PAGE (10% gel), transferred to nitrocellulose membranes, and detected by Western blot analysis. Cytochrome *c* was detected in a Western blot with a cytochrome *c*-specific antibody. (B) Quantification of protein bands shown in panel A. The amount of each protein band was quantified by densitometric analysis with UPV software. The efficiency of release of cytochrome *c* from mitochondrial fraction into cytosolic fraction was expressed as a ratio of cytochrome *c* in the cytosolic fraction to that in the mitochondrial fraction.

Fig. 2, the amounts of cytochrome *c* in the cytosolic and mitochondrial fractions were similar in both virus-infected and mock-infected cells at 12 and 24 h p.i. Quantitative analysis of the protein bands showed that the ratios of cytosolic fraction to mitochondrial fraction were around 1 at 12 and 24 h p.i. (Fig. 2B). However, the amounts of cytochrome *c* significantly increased in the cytosolic fraction as compared to the mitochondrial fraction in virus-infected cells at 36 and 48 h p.i. (increase in the ratios of cytosolic to mitochondrial fraction from 1.24 to 5.4 at 36 h p.i. and to 3.45 at 48 h p.i.;  $P < 0.01$ ) (Fig. 2B). Although the amounts of cytochrome *c* also increased in the cytosolic fraction in mock-infected cells at 36 and 48 h p.i., the level of the increase was much lower than those in virus-infected cells during the same period of time (increase in the ratios of cytosolic to mitochondrial fraction from 1.12 to 2.5 and 2.25 at 36 and 48 h p.i., respectively) (Fig. 2B). This result demonstrates that the mitochondrion-mediated apoptosis pathway is activated in MHV-infected oligodendrocytes.

**Overexpression of Bcl-2 and Bcl-xL inhibited MHV-induced oligodendrocyte apoptosis.** To unequivocally establish that the mitochondrial apoptotic pathway is activated by MHV infection, we transfected the plasmids containing the two master antiapoptotic genes (Bcl-2 and Bcl-xL) of the mitochondria

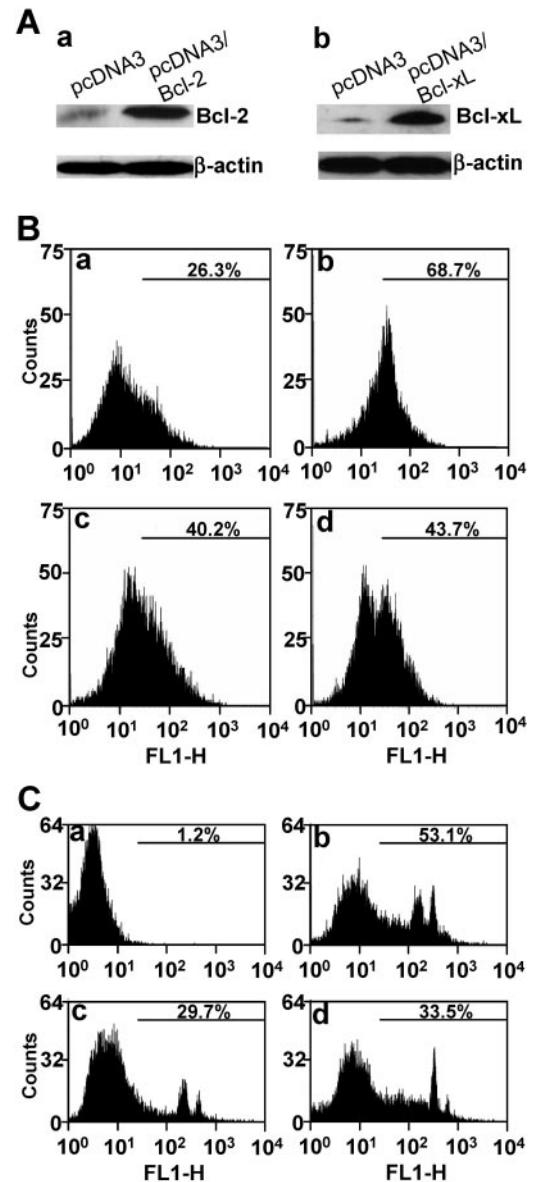


FIG. 3. Inhibition of MHV-induced oligodendrocyte apoptosis by overexpression of Bcl-2 and Bcl-xL. (A) Stable expression of pcDNA3/Bcl-2 (a) and pcDNA3/Bcl-xL (b) in CG-4 cells. Cells transfected with the expression vector alone were used as a negative control (pcDNA3). The expression levels of Bcl-2 and Bcl-xL in the stable cells were determined by Western blot analysis with antibodies specific to Bcl-2 and Bcl-xL, respectively.  $\beta$ -Actin was used as an internal control for normalization of protein amounts. TUNEL (B) and annexin V binding (C) in pcDNA3-transfected and mock-infected oligodendrocytes (a), pcDNA3-transfected and MHV-infected oligodendrocytes (b), pcDNA3/Bcl-2-transfected and MHV-infected oligodendrocytes (c), and pcDNA3/Bcl-xL-transfected and MHV-infected oligodendrocytes (d). TUNEL was performed at 48 h p.i. with the FragEL DNA fragmentation detection kit (Oncogene Research Products), and detection of annexin V binding on the cell surface was carried out at 12 h p.i. with the annexin V-EGFP assay kit (Bio Vision, Inc.). Fluorescence labeling was quantified by flow cytometry, and the percentage of the TUNEL-positive or annexin V-EGFP-positive cells is indicated in each panel. For statistical analysis, data from three independent experiments were analyzed and compared between each pair. FL1-H, fluorescence intensity; counts, cell counts.

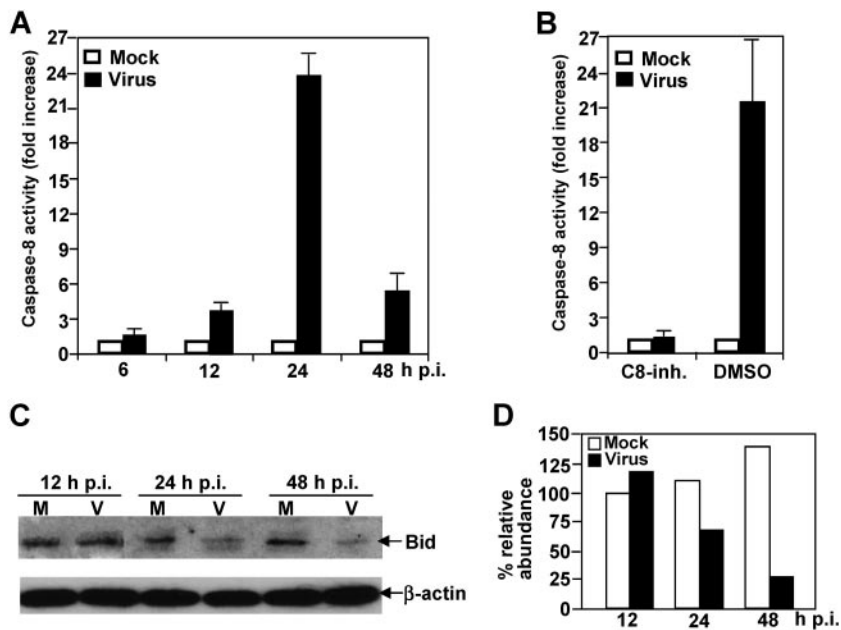


FIG. 4. Activation of caspase-8 and cleavage of proapoptotic protein Bid by MHV infection. (A) Caspase-8 activity. Cells were infected with MHV at an MOI of 5. At various time points p.i. as indicated, cell extract was prepared, and cleavage of pro-caspase-8 and the presence of the active caspase-8 were detected with a caspase colorimetric protease assay kit using specific substrates as described in Materials and Methods. The caspase-8 activity from virus-infected cells was expressed as means  $\pm$  standard error from three independent experiments and as fold increase over that from mock-infected control, which was set as onefold. (B) Effect of caspase-8 inhibitor II on caspase-8 activity. Cells were treated with cell-permeable caspase-8 inhibitor II (C8-inh.) 1 h prior to and during virus infection for 24 h or with DMSO as a negative control. Mock-infected cells were used for normalizing the caspase-8 activity expressed as fold increase as described for panel A. (C) Bid cleavage. Cells were infected with MHV or mock infected with PBS. Cell lysates were collected at various time points p.i. as indicated. The protein level for the full-length Bid was detected by Western blotting using a Bid-specific antibody. The housekeeping protein  $\beta$ -actin was used as an internal control. (D) Quantification of protein bands shown in panel C. The protein bands were quantified by densitometric analysis with UVP software, normalized to  $\beta$ -actin, and expressed as percent relative abundance to Bid of mock-infected cells at 12 h p.i., which was set as 100%.

into the CG-4 cells and established stably expressing cell lines as described previously (15). Figure 3A shows the expression of Bcl-2 and Bcl-xL in CG-4. Cells transfected with the expression vector alone were used as a negative control. When these stably expressing cells were infected with MHV, a significant decrease (approximately 30% reduction) in TUNEL fluorescence staining was detected for both Bcl-2- and Bcl-xL-expressing cells by flow cytometry (Fig. 3B, panels c and d, respectively, for Bcl-2 and Bcl-xL), as compared to that in vector-expressing cells (Fig. 3B, panel b). This difference was statistically significant ( $P < 0.01$ ). However, there were significantly more TUNEL-positive cells in virus-infected and Bcl-2- and Bcl-xL-expressing cells (40 to 45%) than in mock-infected and vector-expressing cells (compare panels c and d with panel a in Fig. 3B;  $P < 0.01$ ). It was noted that there appeared to be two populations for the virus-infected and Bcl-xL-expressing cells (Fig. 3B, panel d). It is possible that one population of cells did not express Bcl-xL and did not protect cells from virus-induced apoptosis, since the Bcl-xL-expressing cells were selected by cell colonies rather than by single-cell clone (15). Nevertheless, these results indicate that the mitochondrial pathway is involved in the induction of oligodendrocyte apoptosis by MHV infection.

To further assess whether the mitochondrial pathway is the primary or secondary pathway induced by MHV infection, we determined the apoptosis at 12 h p.i. by assaying annexin V binding, which is an early indicator of apoptosis. As shown in

Fig. 3C, extensive apoptosis was detected in virus-infected, empty vector-transfected cells (53.1%, panel b) at 12 h p.i.; there was virtually no apoptosis in mock-infected cells (1.2%, panel a). Consistent with the TUNEL experiments, apoptosis was significantly inhibited in cells stably expressing Bcl-2 and Bcl-xL (compare panels c [29.7%] and d [33.5%] for Bcl-2 and Bcl-xL, respectively, with panel b [53.1%];  $P < 0.01$ ). Since inhibition of the mitochondrial pathway by Bcl-2 and Bcl-xL partially blocked apoptosis at an early time point p.i. (12 h p.i.), this result suggests that the mitochondrial pathway is one of the primary pathways induced by MHV infection.

**Activation of caspase-8 activity and cleavage of Bid in MHV-infected oligodendrocytes.** Since the mitochondrial pathway is activated by MHV infection, we further sought to identify the upstream signals that trigger activation of the mitochondrial pathway. It has been well documented in the literature that activation of the mitochondrial apoptotic pathway can be mediated by activation of caspase-8, which in turn mediates cleavage of the proapoptotic protein Bid. Cleaved Bid then translocates to mitochondria and activates the mitochondrial apoptotic pathway. To test this hypothesis, we determined the caspase-8 activity following MHV infection. We found that caspase-8 was activated as early as 12 h p.i. (3.7-fold increase; Fig. 4A). The caspase-8 activity in virus-infected cells reached a plateau ( $\approx 24$ -fold) at 24 h p.i. and then declined to only 5.3-fold by 48 h p.i. in comparison with that of mock-infected cells. This result indicates that caspase-8 is indeed activated by

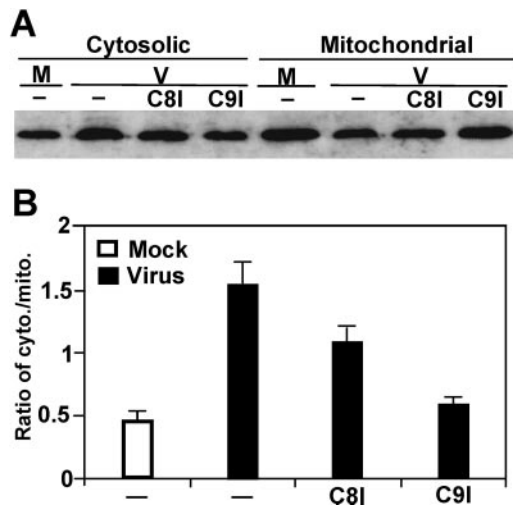


FIG. 5. Effect of caspase-8 and -9 inhibitors on cytochrome *c* release during MHV infection. (A) Cells were treated with caspase-8 or -9 inhibitors 1 h prior to and throughout the infection. At 48 h p.i., cells were lysed. The cytosolic and mitochondrial fractions were separated by differential centrifugation. Cytochrome *c* was detected by Western blotting with a specific antibody as described in the legend to Fig. 2. M, mock infection; V, virus infection; C8I and C9I, caspase-8- and -9 inhibitor, respectively; -, no treatment with caspase inhibitor. (B) Quantification of the protein bands shown in panel A and two additional gels (not shown). The amount of cytochrome *c* was quantified by densitometric analysis with UVP software. The efficiency of release of cytochrome *c* from mitochondria into cytosol is expressed as a ratio of cytosolic fraction to mitochondrial fraction and as means  $\pm$  SD.

MHV infection. To further confirm the specificity of the enzymatic assay, we used a caspase-8 inhibitor (80  $\mu$ M) to treat cells. When cells were treated with the caspase-8 inhibitor prior to and during virus infection, caspase-8 activity was no longer detectable at 24 h p.i. In contrast, when cells were mock treated with DMSO, caspase-8 activity remained at a high level at 24 h p.i. (Fig. 4B).

To further establish the linkage between caspase-8 activation and mitochondrion activation, we determined the cleavage of Bid in virus-infected cells. As shown in Fig. 4C, Bid cleavage indeed occurred in virus-infected cells but not in mock-infected cells at 24 h p.i. Bid cleavage continued to occur at 36 and 48 h p.i. in virus-infected cells. Figure 4D shows the results obtained from quantitative analysis of the protein gels shown in Fig. 4C, which indicate the abundance of each Bid protein band after normalization with  $\beta$ -actin relative to the Bid band for mock-infected cells at 12 h p.i. It is noted that although we could not detect the cleaved product of Bid, the reduction of the full-length Bid at 24 h p.i. and thereafter was not due to either general protein degradation or translational inhibition by virus infection. This conclusion is supported with the following evidence. First, lysates from equivalent numbers of mock-infected and virus-infected cells were analyzed in the Western blot. Second, we also used equivalent protein contents determined by spectrophotometry. Third, the housekeeping protein  $\beta$ -actin exhibited a similar level in both mock- and virus-infected cells. Therefore, the decrease in abundance of the full-length Bid is likely the result of cleavage mediated by the activation of caspase-8.

**Effect of caspase-8 and -9 inhibitors on cytochrome *c* release from mitochondria.** The above results suggest that caspase-8 is a signal upstream of the mitochondria, whereas caspase-9 is probably a downstream signal of mitochondria. To establish that this signaling cascade is operational in MHV-induced apoptosis, cells were treated with caspase-8 or -9 inhibitors prior to and throughout the infection. At 48 h p.i., cells were lysed and cytosolic and mitochondrial fractions were separated by differential centrifugation. Cytochrome *c* was then detected by Western blotting with a specific antibody. As shown in Fig. 5A, treatment of cells with both caspase inhibitors reduced the cytochrome *c* release from mitochondria in virus-infected cells. However, the reduction of cytochrome *c* release was greater in cells treated with caspase-9 inhibitor (63% reduction) than in those treated with caspase-8 inhibitor (30% reduction), although the reduction by both inhibitors was reproducible in three independent experiments and was statistically significant ( $P < 0.01$ ) (Fig. 5B). These results indicate that activation of caspase-8 by MHV infection is not the only upstream signal that triggers the mitochondrial apoptotic pathway and that caspase-9 may also act upon mitochondria to trigger the release of cytochrome *c*.

**Early activation of proapoptotic protein Bax but not Bad by MHV infection.** To further search for upstream signals other than caspase-8 that may trigger the mitochondrial pathway in MHV-induced oligodendrocyte apoptosis, we performed Western blot analysis to detect a number of mitochondrion-associated proapoptotic proteins in cell lysates using specific antibodies. As shown in Fig. 6A, the proapoptotic protein Bax was significantly increased in virus-infected cells as compared to mock-infected cells at 12 h p.i. The increase was more pronounced in virus-infected cells at 24 and 48 h p.i., whereas the level of Bax remained relatively similar throughout the first 24 h p.i. in mock-infected cells, although it increased at 48 h p.i. In contrast, there was no apparent change in Bad expression with virus infection at 12 and 24 h p.i., although an increase was noticeable at 48 h p.i. in virus-infected cells as compared with that in mock-infected cells. These results indicate that up-regulation of Bax by MHV infection is likely one of the upstream signals that trigger the mitochondrial apoptotic pathway, while the late increase in Bad might be the consequence of the apoptotic process.

To establish the functional relevance of the activation of Bax to apoptosis induction, we determined the translocation of Bax to mitochondria following virus infection. Cells were infected with MHV at an MOI of 5. At various time points p.i., cytosolic and mitochondrial fractions were separated by differential centrifugation. Western blotting was performed to detect the presence of Bax. As shown in Fig. 6B, Bax was indeed significantly translocated to the mitochondria in virus-infected cells at 12, 24, and 48 h p.i., whereas no apparent mitochondrial translocation of Bax was detected in mock-infected cells at 12 and 24 h p.i., although Bax translocation was slightly increased at 48 h p.i. in mock-infected cells.

To further determine the signaling cascade of Bax activation and translocation by MHV infection, cells were infected with live virus or UV-irradiated virus or were mock infected for 48 h in the presence or absence of the caspase-8 inhibitor. Cell lysates were then determined for the presence of Bax by Western blot analysis. It was found that both live virus and UV-

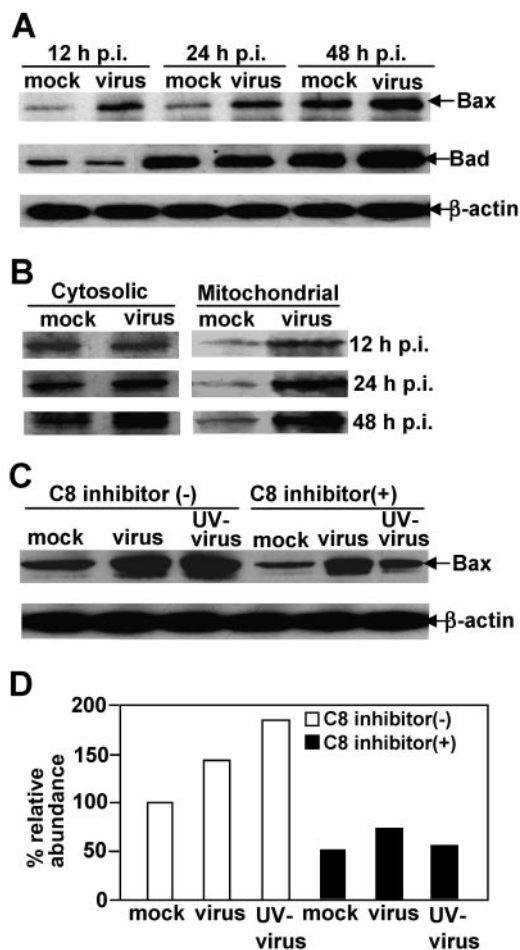


FIG. 6. Early activation of proapoptotic protein Bax but not Bad by MHV-infection. (A) Cells were infected with MHV at an MOI of 5 (virus) or mock infected with PBS (mock). At various time points p.i., as indicated at the top of the figure, cells were harvested and lysed with radioimmunoprecipitation assay buffer. Proteins were separated by SDS-PAGE (12% gel), transferred to nitrocellulose membranes, and detected by Western blot analysis with specific antibodies to Bax, Bad, and  $\beta$ -actin, the latter of which serves as an internal control for normalization of protein amount. The specific protein band is indicated with an arrow on the right. (B) Bax translocation to mitochondria induced by virus infection. The experiments for virus infection and protein detection were the same as those described for panel A, except the cytosolic and mitochondrial fractions were separated from the cell lysates prior to protein analysis. (C) Effect of caspase-8 inhibitor on Bax activation. Cells were treated with the caspase-8 inhibitor or mock treated with DMSO 1 h prior to and throughout the infection and were infected with live virus or UV-inactivated virus or mock infected with PBS. The presence of Bax protein was then detected at 48 h p.i. by Western blotting as described for panel A.  $\beta$ -Actin was used as an internal control for normalization of protein concentration. Arrows on the right indicate the appropriate protein bands. (D) Quantification of the protein bands for Bax shown in panel C. The amount of Bax was quantified by densitometric analysis with UVP software and was expressed as a percentage relative to the Bax band shown in the first lane of panel C (mock infected, untreated with caspase-8 inhibitor).

irradiated virus could induce the expression (Fig. 6C) and translocation of Bax to mitochondria (data not shown). Interestingly, treatment of cells with the caspase-8 inhibitor significantly inhibited Bax expression, suggesting that the activation

of Bax is at least partially through the caspase-8 signaling pathway. Furthermore, the inhibitory effect of the caspase-8 inhibitor on Bax activation was much more pronounced in cells infected with UV-irradiated virus (69% reduction) than in those infected with live virus (47%) (Fig. 6D). This may indicate that Bax activation is likely mediated via both caspase-8-dependent and -independent pathways.

DISCUSSION

In this study, we have demonstrated activation of caspase-9, release of cytochrome *c* from mitochondria, and inhibition of apoptosis by treatment with the caspase-9 inhibitor and by overexpression of Bcl-2 and Bcl-xL, thus establishing the involvement of the mitochondrial apoptotic pathway in oligodendrocyte apoptosis mediated by MHV infection. The mechanism by which MHV infection induces oligodendrocyte apoptosis is currently unknown. Our results offer two potential mechanisms. One is activation of the caspase-8 apoptotic pathway by MHV infection, which is supported by the following lines of evidence. First, activation of caspase-8 appears faster than that of caspase-9. Caspase-8 activity was approximately twofold higher than caspase-9 activity at earlier time points (12 and 24 h p.i.) (Fig. 1 and 4), suggesting that caspase-8 might be an upstream signal of caspase-9. Although the difference in activation of the caspases was statistically not significant at 12 h p.i. ( $P > 0.05$ ), it was very significant at 24 h p.i. ( $P < 0.01$ ). Second, Bid cleavage occurs at 24 h p.i., indicating that the apoptotic signal can be conveyed from the caspase-8 pathway to the mitochondrial pathway via the cleavage and translocation of Bid (Fig. 4C and D). Treatment of cells with the caspase-8 inhibitor prior to virus infection blocked Bid cleavage (data not shown). Third, treatment of cells with the caspase-8 inhibitor that completely inhibited caspase-8 activity (Fig. 4B) inhibited cytochrome *c* release from mitochondria by 30% (Fig. 5), demonstrating the involvement of caspase-8 pathway in activation of the mitochondrial apoptotic pathway. In general, activation of caspase-8 is mediated by cell surface molecules: i.e., through Fas or Fas ligand or TNFR or TNF. It is possible that MHV activates caspase-8 during cell entry. This interpretation is consistent with our previous finding that infection with UV-inactivated MHV is sufficient to induce oligodendrocyte apoptosis (16). Thus, these results suggest that activation of the mitochondrial pathway might be the secondary event following the caspase-8 pathway. However, this is in contrast to MHV-induced apoptosis in the fibroblast cell line 17CL-1, in which virus replication is required and activation of the caspase-8 pathway is dependent on activation of the mitochondrial pathway (3).

The other possible mechanism suggested from our current findings is that MHV-induced oligodendrocyte apoptosis is mediated through the mitochondrial signal pathway independent of the caspase-8 activation. Although treatment of cells with caspase-8 inhibitor completely blocked activation of caspase-8 (Fig. 4B), release of cytochrome *c* from mitochondria was only partially inhibited (Fig. 5B). This suggests that signals other than caspase-8 activation might have activated the cytochrome *c* release. One such upstream candidate is likely Bax, a proapoptotic member of the Bcl-2 family. Indeed, Bax was significantly activated at 12 h p.i. and remained so

throughout the period of 48 h p.i. It has been well established that once activated, Bax translocates to mitochondria (Fig. 6B) to interact with antiapoptotic members such as Bcl-2 and Bcl-xL, thus shifting the balance to apoptotic. How Bax is activated in oligodendrocytes by MHV infection at this early time is an intriguing question. In a variety of cell types, activation of Bax is usually mediated by intracellular apoptotic signals such as DNA damage, p53 activation, or virus replication. However, induction of the oligodendrocyte apoptosis described here does not require virus replication since infection with the UV-inactivated virus can sufficiently induce apoptosis (16). One possible explanation is that a common upstream apoptotic signal localizes at, or in the vicinity of, the cytoplasm membrane of oligodendrocytes. This signal is triggered by virus infection during entry into cells, which in turn triggers the activation of caspase-8 and also other molecules that activate downstream signals such as Bax. Indeed, Bax was activated by infection with UV-inactivated virus (Fig. 6C), and its activation was partially inhibited by treatment with the caspase-8 inhibitor. Alternatively, since the inhibition of Bax activation was more pronounced in cells infected with UV-inactivated virus than in those infected with live virus (Fig. 6C and D), it is possible that virus replication, though not required for apoptosis induction, also contributes partially to the activation of Bax expression and consequently to the release of cytochrome *c* from the mitochondria, which is independent of the activation of caspase-8 (8). In addition, overexpression of Bcl-2 and Bcl-xL significantly inhibited MHV-induced apoptosis (Fig. 3B and C), even when the apoptosis was measured at an early time point (12 h p.i.). This finding suggests that the mitochondrial signaling might be one of the primary apoptotic pathways that are induced by MHV infection. Interestingly, in contrast to the TUNEL results obtained at 48 h p.i. (Fig. 3B, panel b), the results from annexin V staining at 12 h p.i. showed two distinct subpopulations of annexin V-positive cells (Fig. 3C, panel b), and only one subpopulation appeared to be predominantly inhibited by overexpression of Bcl-2 and Bcl-xL (Fig. 3C, panels c and d). These findings support the argument that the apoptosis of one subpopulation of the cells is likely mediated through the mitochondrial signaling pathway and that the mitochondrial pathway is likely the primary rather than the secondary pathway, partially responsible for MHV-induced oligodendrocyte apoptosis.

Our results raise another interesting issue regarding the signaling cascade. Activation of caspase-9 is usually triggered by the release of cytochrome *c* from mitochondria and the interaction with the cytochrome *c*/Apaf-1 complex. As such, a downstream signal (caspase-9 activity) should not have an effect on its upstream signal (cytochrome *c* release) in the mitochondrial apoptotic signaling cascade. However, when cells were treated with the caspase-9 inhibitor, not only was caspase-9 activity completely blocked but the release of cytochrome *c* from mitochondria was severely impaired (Fig. 5). These results suggest that caspase-9 may have an ability to feed forward activation of the mitochondrial pathway. Although the mechanism for such a feed-forward regulation by caspase-9 is currently unknown, a similar phenomenon has been described previously (8). Studies have shown that cytochrome *c* release and caspase-9 activation can occur before the loss of mitochondrial inner transmembrane potential ( $\Delta\psi_m$ ) and the opening of

a large conductance channel known as the mitochondrial permeability transition pore (2, 26). Activation of caspases can induce permeability transition pore opening (17, 25), which in turn can induce cytochrome *c* release from the mitochondria and caspase-9 activation. This kind of regulation represents a feed-forward amplification loop of the apoptotic cascades (8). Thus, identification of the apoptotic signaling pathways in oligodendrocytes will provide insight into the mechanisms by which MHV infection causes oligodendrocyte destruction and demyelination in the CNS.

#### ACKNOWLEDGMENTS

This work was supported by a grant from the National Institutes of Health (NS47499).

We thank Marie Hardwick (Johns Hopkins University) for kindly providing the Bcl-2 plasmid and Kelli Halcom (X. Zhang's laboratory) for proofreading the manuscript.

#### REFERENCES

1. Barac-Latas, V., G. Suchanek, H. Breitschopf, A. Stuehler, H. Wege, and H. Lassmann. 1997. Patterns of oligodendrocyte pathology in coronavirus-induced subacute demyelinating encephalomyelitis in the Lewis rat. *Glia* **19**: 1–12.
2. Bossy-Wetzell, E., D. D. Newmeyer, and D. R. Green. 1998. Mitochondrial cytochrome *c* release in apoptosis occurs upstream of DEVD-specific caspase activation and independently of mitochondrial transmembrane depolarization. *EMBO J.* **17**:37–49.
3. Chen, C. J., and S. Makino. 2002. Murine coronavirus-induced apoptosis in 17Cl-1 cells involves a mitochondria-mediated pathway and its downstream caspase-8 activation and bid cleavage. *Virology* **302**:321–332.
4. Cohen, G. M. 1997. Caspases: the executioners of apoptosis. *Biochem. J.* **326**:1–16.
5. Dandekar, A. A., and S. Perlman. 2002. Virus-induced demyelination in nude mice is mediated by gamma delta T cells. *Am. J. Pathol.* **161**:1255–1263.
6. Das Sarma, J., L. Fu, J. C. Tsai, S. R. Weiss, and E. Lavi. 2000. Demyelination determinants map to the spike glycoprotein gene of coronavirus mouse hepatitis virus. *J. Virol.* **74**:9206–9213.
7. Fleming, J. O., F. I. Wang, M. D. Trousdale, D. R. Hinton, and S. A. Stohman. 1993. Interaction of immune and central nervous systems: contribution of anti-viral Thy-1+ cells to demyelination induced by coronavirus JHM. *Reg. Immunol.* **5**:37–43.
8. Green, D. R., and J. C. Reed. 1998. Mitochondria and apoptosis. *Science* **281**:1309–1312.
9. Hirano, N., K. Fujiwara, S. Hino, and M. Matumoto. 1974. Replication and plaque formation of mouse hepatitis virus (MHV-2) in mouse cell line DBT culture. *Arch. Gesamte Virusforsch.* **44**:298–302.
10. Houtman, J. J., and J. O. Fleming. 1996. Pathogenesis of mouse hepatitis virus-induced demyelination. *J. Neurovirol.* **2**:361–376.
11. Hsu, H., H. B. Shu, M. G. Pan, and D. V. Goeddel. 1996. TRADD-TRAF2 and TRADD-FADD interactions define two distinct TNF receptor 1 signal transduction pathways. *Cell* **84**:299–308.
12. Kelekar, A., B. S. Chang, J. E. Harlan, S. W. Fesik, and C. B. Thompson. 1997. Bad is a BH3 domain-containing protein that forms an inactivating dimer with Bcl-x<sub>L</sub>. *Mol. Cell. Biol.* **17**:7040–7046.
13. Knobler, R. L., M. V. Haspel, M. Dubois-Dalcq, P. W. Lampert, and M. B. Oldstone. 1981. Host and virus factors associated with CNS cellular tropism leading to encephalomyelitis or demyelination induced by the JHM strain of mouse hepatitis virus. *Adv. Exp. Med. Biol.* **142**:341–348.
14. Lavi, E., D. H. Gilden, M. K. Highkin, and S. R. Weiss. 1984. Persistence of mouse hepatitis virus A59 RNA in a slow virus demyelinating infection in mice as detected by in situ hybridization. *J. Virol.* **51**:563–566.
15. Liu, Y., and X. Zhang. 2005. Expression of cellular oncogene Bcl-xL prevents coronavirus-induced cell death and converts acute infection to persistent infection in progenitor rat oligodendrocytes. *J. Virol.* **79**:47–56.
16. Liu, Y., Y. Cai, and X. Zhang. 2003. Induction of caspase-dependent apoptosis in cultured rat oligodendrocytes by murine coronavirus is mediated during cell entry and does not require virus replication. *J. Virol.* **77**:11952–11963.
17. Marzo, I., C. Brenner, N. Zamzami, S. A. Susin, G. Beutner, D. Brdiczka, R. Remy, Z. H. Xie, J. C. Reed, and G. Kroemer. 1998. The permeability transition pore complex: a target for apoptosis regulation by caspases and bcl-2-related proteins. *J. Exp. Med.* **187**:1261–1271.
18. McNulty, S., M. Crouch, D. Smart, and M. Rumsby. 2001. Differentiation of bipolar CG-4 line oligodendrocytes is associated with regulation of CREB, MAP kinase and PKC signalling pathways. *Neurosci. Res.* **41**:217–226.
19. Nijhawan, D., N. Honarpour, and X. Wang. 2000. Apoptosis in neural development and disease. *Annu. Rev. Neurosci.* **23**:73–87.

20. Roulston, A., R. C. Marcellus, and P. E. Branton. 1999. Viruses and apoptosis. *Annu. Rev. Microbiol.* **53**:577–628.
21. Schwartz, T., L. Fu, and E. Lavi. 2002. Differential induction of apoptosis in demyelinating and nondemyelinating infection by mouse hepatitis virus. *J. Neurovirol.* **8**:392–399.
22. Sedlak, T. W., Z. N. Oltvai, E. Yang, K. Wang, L. H. Boise, C. B. Thompson, and S. J. Korsmeyer. 1995. Multiple Bcl-2 family members demonstrate selective dimerizations with Bax. *Proc. Natl. Acad. Sci. USA* **92**:7834–7838.
23. Stohlman, S. A., C. C. Bergmann, and S. Perlman. 1999. Mouse hepatitis virus, p. 537–557. *In* R. Ahmed and I. Chen (ed.), *Persistent viral infections*. Wiley, New York, N.Y.
24. Strasser, A., L. O'Connor, and V. M. Dixit. 2000. Apoptosis signaling. *Annu. Rev. Biochem.* **69**:217–245.
25. Susin, S. A., N. Zamzami, M. Castedo, E. Daugas, H. G. Wang, S. Geley, F. Fassy, J. C. Reed, and G. Kroemer. 1997. The central executioner of apoptosis: multiple connections between protease activation and mitochondria in Fas/APO-1/CD95- and ceramide-induced apoptosis. *J. Exp. Med.* **186**:25–37.
26. Vander Heiden, M. G., N. S. Chandel, E. K. Williamson, P. T. Schumacker, and C. B. Thompson. 1997. Bcl-xL regulates the membrane potential and volume homeostasis of mitochondria. *Cell* **91**:627–637.
27. Vaux, D. L., S. Cory, and J. M. Adams. 1988. Bcl-2 gene promotes haemopoietic cell survival and cooperates with c-myc to immortalize pre-B cells. *Nature* **335**:440–442.
28. Wang, F. I., S. A. Stohlman, and J. O. Fleming. 1990. Demyelination induced by murine hepatitis virus JHM strain (MHV-4) is immunologically mediated. *J. Neuroimmunol.* **30**:31–41.
29. Wang, K., X. M. Yin, D. T. Chao, C. L. Milliman, and S. J. Korsmeyer. 1996. BID: a novel BH3 domain-only death agonist. *Genes Dev.* **10**:2859–2869.
30. Wu, G. F., A. A. Dandekar, L. Pewe, and S. Perlman. 2000. CD4 and CD8 T cells have redundant but not identical roles in virus-induced demyelination. *J. Immunol.* **165**:2278–2286.
31. Wu, G. F., and S. Perlman. 1999. Macrophage infiltration, but not apoptosis, is correlated with immune-mediated demyelination following murine infection with a neurotropic coronavirus. *J. Virol.* **73**:8771–8780.
32. Wyllie, A. H. 1980. Glucocorticoid-induced thymocyte apoptosis is associated with endogenous endonuclease activation. *Nature* **284**:555–556.
33. Yang, E., J. Zha, J. Jockel, L. H. Boise, C. B. Thompson, and S. J. Korsmeyer. 1995. Bad, a heterodimeric partner for Bcl-XL and Bcl-2, displaces Bax and promotes cell death. *Cell* **80**:285–291.
34. Yeh, J. H., S. C. Hsu, S. H. Han, and M. Z. Lai. 1998. Mitogen-activated protein kinase kinase antagonized fas-associated death domain protein-mediated apoptosis by induced FLICE-inhibitory protein expression. *J. Exp. Med.* **188**:1795–1802.